This paper first appeared in the fifteenth print edition of the *Photovoltaics International* journal, published in February 2012.

Firing stability of SiN_y/SiN_x and Al_2O_3/SiN_x stacks for the rear-surface passivation of industrial-type crystalline silicon solar cells

Sebastian Gatz[1], **Jan Schmidt**[1,2], **Boris Veith**[1], **Thorsten Dullweber**[1] & **Rolf Brendel**[1,2]
[1]Institute for Solar Energy Research Hamelin (ISFH), Emmerthal; [2]Institute of Solid-State Physics, Leibniz University of Hanover (LUH), Hanover, Germany

ABSTRACT

In the photovoltaics industry, contacts to crystalline silicon are typically formed by the firing of screen-printed metal pastes. However, the stability of dielectric surface passivation layers during the high-temperature contact formation has turned out to be a major challenge for some of the best passivating layers, such as intrinsic amorphous silicon. Capping of well-passivating dielectric layers by hydrogen-rich silicon nitride (SiN_x), however, has been demonstrated to improve the thermal stability, an effect which can be attributed to the atomic hydrogen (H) diffusing out to the interface during firing, and passivating dangling bonds. This paper presents the results of investigations into the influence of two different dielectric passivation stacks on the firing stability, namely SiN_y/SiN_x ($y < x$) and Al_2O_3/SiN_x stacks. Excellent firing stability was demonstrated for both stack systems. Effective surface recombination velocities of < 10cm/s were measured after a conventional co firing process on 1.5Ωcm *p*-type float-zone silicon wafers for both passivation schemes. On the solar cell level, however, better results were obtained using the Al_2O_3/SiN_x stack, where an efficiency of 19.6% was achieved for a large-area screen-printed solar cell fabricated on conventional Czochralski-grown silicon.

Introduction

Industrial crystalline sillicon solar cells typically feature a full-area aluminium (Al) back-surface field (BSF) at the rear. This provides an ohmic contact and a moderate rear-surface passivation, with effective rear-surface recombination velocities S_{rear} ranging from 400 to 600cm/s on 2–4Ωcm *p*-type silicon. In order to increase cell efficiency, the passivation quality and the internal reflectivity at the rear need to be improved. These two requirements are fulfilled in the passivated emitter and rear solar cell (PERC) concept [1], which is schematically shown in Fig. 1(a).

> "In order to increase cell efficiency, the passivation quality and the internal reflectivity at the rear need to be improved."

In the PERC approach, screen-printed Al paste is deposited on the complete rear surface on top of locally opened dielectric rear-surface passivation layers. During a co-firing step in an industrial infrared beltline furnace, not only is a local BSF formed in the opened areas, but also the homogeneous phosphorous-doped emitter at the front is contacted by a screen-printed silver (Ag) paste. A thermally grown silicon dioxide layer exhibits an excellent firing-stable surface passivation. However, the low-throughput furnace process is disadvantageous for industrial applications. The described PERC process imposes some additional requirements on the passivation system at the rear:

- Thermal stability of surface passivation in order to withstand the high-temperature co-firing step
- High optical reflectivity in the infrared wavelength range
- No parasitic shunting at the rear contacts [2]

The one-dimensional device simulation [3] depicted in Fig. 1(b) shows that the effective surface recombination velocity in the passivated regions S_{pass} has a strong impact on the solar cell efficiency η. The surface recombination velocity in the metallized regions S_{met} is around 600cm/s [4]. In order to improve the conversion efficiency of about 18.5% for conventional solar cells with a full-area Al-BSF, it is essential to provide a passivation featuring

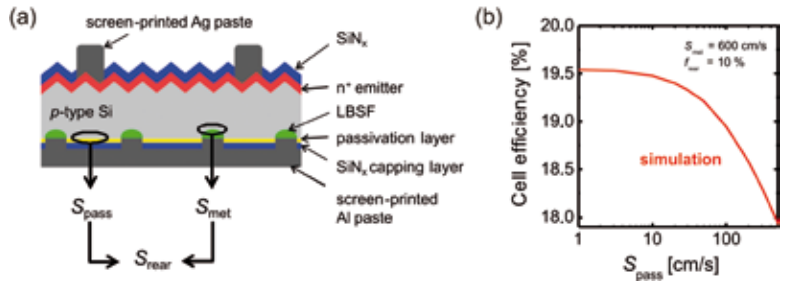

Figure 1. (a) Schematic of a PERC solar cell applying screen-printed Ag front and Al rear contacts with local openings in the passivation stack. The electrical quality of the rear is characterized by the effective surface recombination velocity S_{rear}, which is influenced by the surface recombination velocities in the dielectric passivated areas S_{pass} and in the metallized contact areas S_{met}. (b) PC1D simulation of the energy conversion efficiency as a function of S_{pass} for a PERC solar cell on boron-doped Cz-silicon with a resistivity of 2.1Ωcm.

S_{pass} values below 100cm/s. However, the simulation reveals a saturation of the possible conversion efficiency at around 19.5% for S_{pass} values under 20cm/s.

Because of the high throughput, the plasma-enhanced chemical vapour deposition (PECVD) technique for the surface passivation offers the possibility of reducing costs. For silicon nitride (SiN_x) layers, the surface passivation quality and firing stability are highly dependent on the composition and therefore on the refractive index n of the dielectric [5,6]. A value of $n \approx 2.5$ results in low effective surface recombination velocities S_{pass} for the as-deposited state, whereas a layer with $n \approx 2.05$ performs best after a firing step in the temperature range of 800 to 900°C [7]. The latter configuration is used, for example, with conventional screen-printed solar cells for passivating the phosphorus-diffused emitter at the front [6]. The passivation of these SiN_x films, deposited in an NH_3-rich gas mixture, relies mainly on the field-effect passivation provided by a high density of fixed positive charges in the insulating SiN_x films [8]. Additionally, the surfaces are passivated by atomic hydrogen (H) released from the precursor gases during the PECVD deposition. However, parasitic shunting between the back contacts and the inversion layer underneath the SiN_x interface has been found to degrade the cell performance for p-type surfaces [2].

Intrinsic amorphous silicon (a-Si) films deposited on crystalline silicon exhibit only small, if any, charge densities and therefore do not cause parasitic shunting [9]. If the dangling bonds at the interface are saturated with hydrogen which is released during PECVD deposition, these a-Si films provide the same low S_{pass} values as thermally grown SiO_2 [10–14]. But applying temperatures above 400°C severely deteriorates the passivation quality [15]. Depositing a SiN_x capping layer with $n_{SiNx} \approx 2.05$ on top of the a-Si layer not only protects the a-Si layer from the Al rear metallization but also improves the thermal stability of the surface passivation [14,16,17]. However, the a-Si/SiN_x stacks were shown to be stable only for firing temperatures $T \leq 750$°C. When standard firing temperatures between 800 and 900°C are applied, the surface passivation severely deteriorates. In this paper, it is shown that the addition of small amounts of nitrogen to the a-Si layer, resulting in SiN_y/SiN_x stacks with $y < x$, improves the firing stability of the stacks significantly.

Another dielectric layer which provides an excellent level of surface passivation is aluminium oxide (Al_2O_3). With laboratory PERC cells, Al_2O_3 has been demonstrated to prevent any parasitic shunting because of its high negative fixed charge density that is responsible for the excellent field-effect passivation [18]. During firing, however, the high level of surface passivation provided by single Al_2O_3 layers deteriorates, an effect which is attributed to a release of interfacial hydrogen. It has recently been shown that the firing stability is significantly improved for Al_2O_3/SiN_x stacks compared to single layers of Al_2O_3 [19,20]. In the present paper, both types of industrially-relevant passivation stacks – SiN_y/SiN_x and Al_2O_3/SiN_x – are directly compared on the basis of lifetime as well as solar cell results.

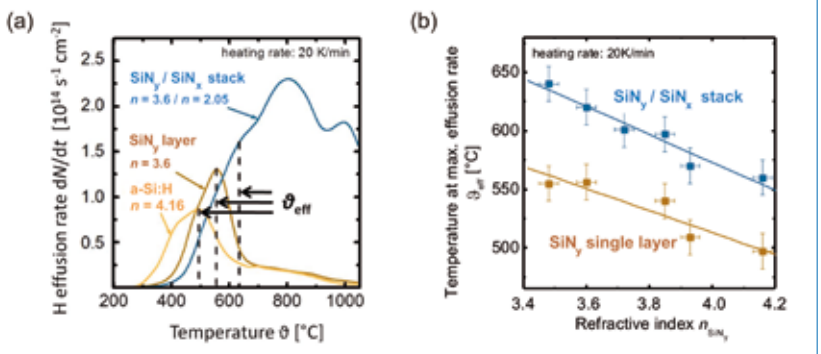

Figure 2. (a) H effusion rate as a function of the measured temperature. The characteristic effusion temperatures ϑ_{eff} are related to the respective maximal H effusion rate from the passivating film. (b) Effusion temperatures ϑ_{eff} from the SiN_y passivation layer increase with decreasing n_{SiNy} for both SiN_y single and SiN_y/SiN_x stack layers. The increase in ϑ_{eff} using a SiN_x capping layer indicates the further reduction of H effusion. The dashed lines are guides for the eye. (Data are taken from Gatz et al. [24].)

SiN_y/SiN_x passivation stacks

The influence of SiN_y/SiN_x passivation stacks on the firing stability with a silicon-rich SiN_y passivation layer and a nitrogen-rich SiN_x capping layer is investigated. The main idea is to increase the thermal stability of the surface passivation by supplying minor amounts of NH_3 during the a-Si deposition in order to reduce hydrogen effusion during a conventional screen-printing firing process. Moreover, it is known that the positive charge density, responsible for the parasitic shunting, is substantially reduced if the nitrogen content of the amorphous film is low [21,22].

In SiN_y, hydrogen is bonded in an amorphous silicon nitride network. Thermally stimulated hydrogen diffuses out of the PECVD layers, and is therefore no longer available for passivating the silicon surface. This was shown by hydrogen effusion experiments [23], which revealed information about the hydrogen content and the thermal stability of hydrogen bonds. During effusion our samples are annealed in vacuum with a heating rate of 20K/min. Hydrogen atoms and molecules that diffuse out of the PECVD layers are detected in real time by means of a mass spectrograph. For an a-Si single layer, a hydrogen effusion peak at a characteristic temperature (ϑ_{eff}) is expected, which is a measure of the thermal stability of the hydrogen in the a- Si layer.

Fig. 2(a) shows measured effusion rates for various passivation layers. The hydrogen effusion rate of an a-Si single layer starts to increase at temperatures of about 300°C and reveals a peak at ϑ_{eff}, the characteristic effusion temperature, equal to 495°C. For the SiN_y single layer with n = 3.6 the temperature at which hydrogen effusion starts and the value of ϑ_{eff} have both increased. When a 100nm-thick SiN_x capping layer is deposited on top of the SiN_y layer, the bend in the curve of the effusion rate at $\vartheta_{eff} \approx 630$°C can be attributed to the hydrogen diffusing out of the SiN_y passivation layer. Effusion peaks at temperatures of approximately 800°C and 1000°C are found to be typical for the SiN_x capping layer.

Fig. 2(b) shows ϑ_{eff} for single and double passivation layers as a function of the real part of the refractive index n of the 10nm-thick passivation layers. ϑ_{eff} decreases continuously from 550°C for SiN_y single layers (n = 3.48) to 495°C for an a-Si single layer (n = 4.16). The diffusing out of hydrogen is reduced because of the presence of nitrogen. It is concluded from FTIR measurements that this is due to the larger bonding strength of hydrogen with an increasing concentration of Si-N back bonds (as demonstrated by Gatz et al. [24]). In addition, Fig. 2(b) shows that, if a SiN_x capping layer is applied, the peak temperature increases by 60 to 90°C for all SiN_y layers. A reduced hydrogen effusion rate due to a SiN_x capping layer has already been reported in the literature [25].

The following discussion will focus on carrier lifetime investigations of SiN_y/SiN_x passivated crystalline Si surfaces. The effective lifetime τ_{eff} of symmetrically passivated p-type FZ Si

wafers is measured by means of the quasi-steady-state photoconductance (QSSPC) method [26,27]. If the total measured recombination rate is attributed to the interface, the upper limit for the effective surface recombination velocity can be estimated from the equation

$$S_{pass} = \frac{W}{2 \cdot \tau_{eff}} \quad (1)$$

where τ_{eff} is effective lifetime measured by QSSPC and W is the wafer thickness.

The effective surface recombination velocity S_{pass} before and after firing in an infrared conveyor-belt furnace for SiN_y/SiN_x double layers is shown in Fig. 3. S_{pass} in the as-deposited state decreases slightly with increasing refractive index from about 22cm/s (n = 3.14) to 8cm/s (n = 4.16). The firing step alters the S_{pass} dependence significantly. A minimum of S_{pass} occurs for n in the range of n = 3.4 to 3.8 with the minimum upper limit S_{eff} = (10±2)cm/s for stacks with n = 3.6. After firing, as the refractive index increases further towards $n_{a\text{-}Si}$ = 4.16, S_{pass} increases significantly due to the reduced bonding strength of H in the SiN_y film, as indicated by our FTIR and H effusion results. With optimization of the process gas composition, S_{pass} remains below 10cm/s at relevant injection densities of the solar cell between $\Delta n = 10^{13}cm^{-3}$ and $\Delta n = 10^{15}cm^{-3}$ (as has been shown by Gatz et al. [24]).

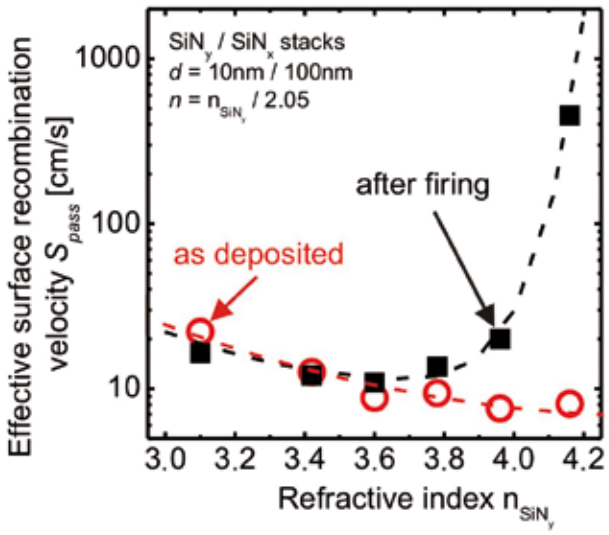

Figure 3. Effective surface recombination velocity S_{pass} at $\Delta n = 10^{15}cm^{-3}$ before and after a firing step as a function of the passivation layer's refractive index n for SiN_y/SiN_x stacked layers. The dashed lines are guides for the eye. (Data are taken from Gatz et al. [24].)

Al_2O_3/SiN_x passivation stacks

Fig. 4 shows the effective surface recombination velocity S_{pass}, at a fixed injection density of $10^{15}cm^{-3}$ after firing in a belt furnace, as a function of the Al_2O_3 layer thickness. The Al_2O_3 layers were deposited by two variants of atomic layer deposition (ALD): (a) plasma-assisted ALD (PA-ALD), and (b) thermal ALD.

> "Both PA-ALD-Al_2O_3 and thermal ALD-Al_2O_3 stacks are well suited to application to high-efficiency screen-printed PERC solar cells."

For PA-ALD-Al_2O_3 single layers of thicknesses < 20nm, a pronounced degradation of the effective surface recombination velocity S_{pass} after firing is observed, whereas Al_2O_3/SiN_x stacks with thin Al_2O_3 layers < 20nm show a negligible increase of S_{pass}; there is even an improvement for ultrathin layers ≤ 4nm. For layers of thickness ≥ 20nm, no significant difference is detectable between single layers and Al_2O_3/SiN_x stacks. Both PA-ALD-Al_2O_3 (Fig. 4a) and thermal ALD-Al_2O_3 (Fig. 4b) layers provide approximately the same excellent passivation level, with just slightly lower effective surface recombination velocities for the PA-ALD-Al_2O_3/SiN_x stacks. It is noteworthy that both stack systems with Al_2O_3 layers of thicknesses between 4 and 10nm provide lifetimes between 1 and 3ms after firing, corresponding to surface recombination velocities below 10cm/s over a very broad injection range (10^{13}–$10^{15}cm^{-3}$). Hence, both stacks are well suited to application to high-efficiency screen-printed PERC solar cells.

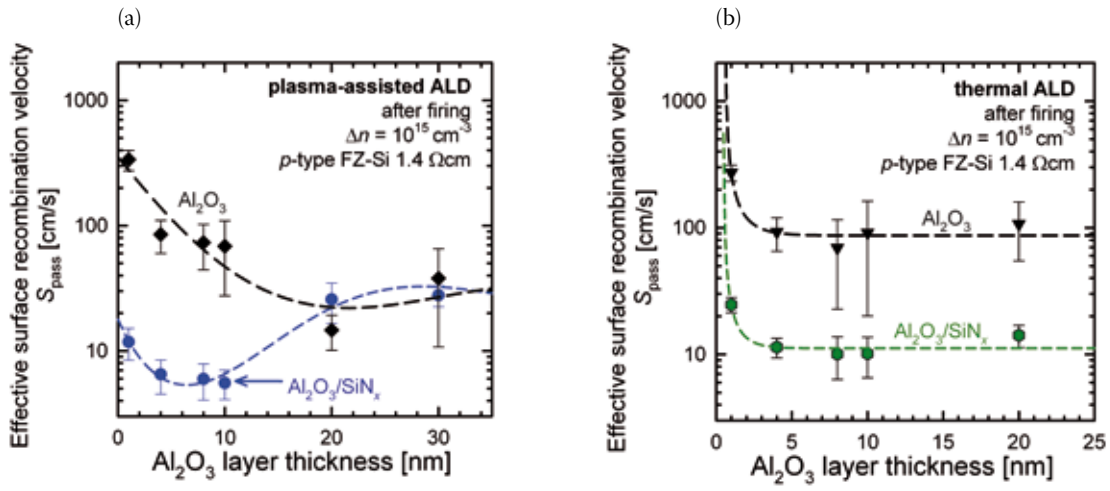

Figure 4. Effective surface recombination velocity as a function of Al_2O_3 layer thickness after firing, for single layers of Al_2O_3 compared with Al_2O_3/SiN_x stacks. The results are shown for Al_2O_3 layers deposited by (a) plasma-assisted ALD, and (b) thermal ALD. The samples received no anneal before firing. The dashed lines are guides for the eye.

Solar cell results

The processing sequence of our screen-printed PERC solar cells is described in Dullweber et al. [28]. Table 1 shows representative measured cell parameters of PERC solar cells with SiN_y/SiN_x (cell type A), plasma-assisted ALD-Al_2O_3/SiN_x (cell type B) and SiO_2/SiN_x (cell type C) rear-surface passivation stacks after the permanent deactivation of the boron-oxygen-related recombination centres [29,30].

> "At the solar cell level, Al_2O_3/SiN_x clearly outperforms SiN_y/SiN_x."

PERC solar cells of types B and C achieve conversion efficiencies of 19.6% and 19.4% [31] compared to 18.3% for cell type A [24]. This difference is related to the open-circuit voltage V_{oc} of 633mV and short-circuit current density J_{sc} of 37.1mA/cm^2 of the SiN_y/SiN_x passivated solar cell, and is mainly attributed to significant improvements in V_{oc} of up to 664mV and in J_{sc} of up to 38.6mA/cm^2. Part of the improvement of cells B and C compared to cell A, however, is due to an improved front-side metallization. The fill factor *FF* does not depend on the passivation, but is strongly related to the metallization fraction at the rear and therefore to the pitch of the rear contacts [32].

Cell type	Area [cm^2]	Rear-surface passivation	Pitch [mm]	V_{oc} [mV]	J_{sc} [mA/cm^2]	*FF* [%]	η [%]
A	141	SiN_y/SiN_x	1	633	37.1	77.8	18.3*
B	233	Al_2O_3/SiN_x	1.2	645	38.6	78.5	19.6**
C	149	SiO_2/SiN_x	2	664	38.5	75.8	19.4**

* in-house measurements at ISFH
** independently confirmed by FhG-ISE CalLab

Table 1. Parameters of solar cells using *p*-type boron-doped Cz-silicon (2.1Ωcm), measured under standard test conditions.

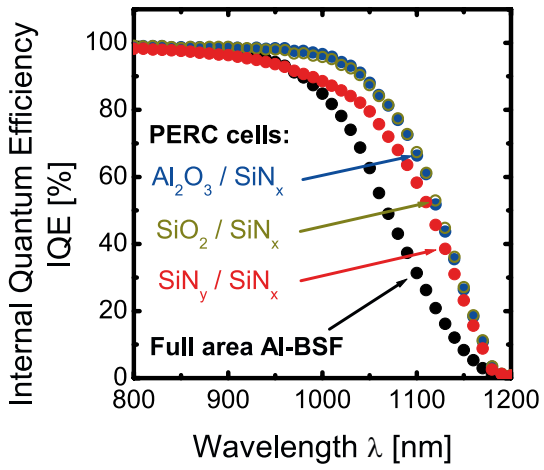

Figure 5. Comparison of measured IQE of the PERC solar cells with Al_2O_3/SiN_x, SiO_2/SiN_x and SiN_y/SiN_x rear-surface passivation stacks and a reference cell with a full-area Al-BSF.

Figure 6. Contact formation of screen-printed solar cells in a conveyor-belt furnace at ISFH.

Fig. 5 shows the measured internal quantum efficiency (IQE) data for the PERC solar cells, as well as for a conventional solar cell featuring a full-area Al-BSF. The effective rear-surface recombination velocity S_{rear} of each solar cell is extracted, along with reflectance data (not shown here), in the wavelength region between 850nm and 1000nm. For cells of types B and C, the analysis leads to S_{rear} < 100cm/s [31]. Assuming S_{met} = 600cm/s for the metallized regions, then S_{rear} < 100cm/s corresponds to S_{pass} < 20cm/s in the passivated areas [4]; that confirms the lifetime measurement results for Al_2O_3/SiN_x (see Fig. 4) and also previous measurement results for SiO_2/SiN_x passivation stacks [33].

A solar cell of type A with SiN_y/SiN_x rear-surface passivation shows an S_{rear} of (400±100)cm/s. This value is slightly smaller than the S_{rear} of about (550±100) cm/s for the solar cell with full-area Al-BSF, indicating that there is only a slightly improved surface passivation quality with the SiN_y/SiN_x stack. However, if it is assumed that S_{met} = 600cm/s for local Al contacts, then S_{rear} = 400cm/s corresponds to $S_{pass} \approx$ 300cm/s in the passivated areas [4]. That value clearly exceeds the S_{pass} < 10cm/s obtained from lifetime measurements. The physical reason for this discrepancy is currently under detailed investigation at ISFH.

Conclusions

As industrially-relevant alternatives to passivation by high-temperature-grown silicon oxide, two different low-temperature passivation schemes have been investigated for rear-surface passivation of screen-printed PERC solar cells: SiN_y/SiN_x (y < x) and Al_2O_3/SiN_x stacks. Both stack layers exhibit an excellent surface passivation quality before and after firing in an industrial conveyor-belt furnace, as demonstrated by effective surface recombination velocities S_{pass} < 10cm/s. However, at the solar cell level, Al_2O_3/SiN_x clearly outperforms SiN_y/SiN_x. When the optimized ISFH screen-printed PERC process is used, energy conversion efficiencies of up to 19.6% are obtained for large-area solar cells with conventional Cz-Si wafers.

References

[1] Blakers, A.W. et al. 1989, "22.8% efficient silicon solar cell", *Appl. Phys. Lett.*, Vol. 55, pp. 1363–1365.

[2] Dauwe, S. et al. 2002, "Experimental evidence of parasitic shunting in silicon nitride rear surface passivated solar cells", *Prog. Photovolt: Res. Appl.*, Vol. 10, No. 4, pp. 271–278.

[3] Clugston, D.A. & Basore, P.A. 1997, "Pc1d version 5: 32-bit solar cell modeling on personal computers", *Proc. 26th IEEE PVSC*, Anaheim, California, USA, pp. 207–210.

[4] Gatz, S. et al. 2011, "Analysis of local Al-doped back surface fields for high-efficiency screen-printed solar cells", *Energy Procedia*, Vol. 8, pp. 318–323.

[5] Lauinger, T., Aberle, A.G. & Hezel, R. 1997, "Comparison of direct and remote PECVD silicon nitride films for low-temperature surface passivation of *p*-type crystalline silicon", *Proc. 14th EU PVSEC*, Barcelona, Spain, pp. 853–856.

[6] Upadhyaya, A., Sheoran, M. & Rohatgi, A. 2005, "Study of direct PECVD SiN_x-induced surface emitter and bulk defect passivation in p-type silicon solar cells", *Proc. 31st IEEE PVSC*, Lake Buena Vista, Florida, USA, pp. 1273–1276.

[7] Lenkeit, B. et al. 2001, "Excellent thermal stability of remote PECVD silicon nitride films for screen-printed bifacial silicon solar cells", *Solar Energy Mater. & Solar Cells*, Vol. 65, pp. 317–323.

[8] Hezel, R. & Jäger, K. 2989, "Low-temperature surface passivation of silicon for solar cells", *J. Electrochem. Soc.*, Vol. 136, pp. 518–523.

[9] Dauwe, S., Schmidt, J. & Hezel, R. 2002, "Very low surface recombination velocities on *p*- and *n*-type silicon wafers passivated with hydrogenated amorphous silicon films", *Proc. 29th IEEE PVSC*, New Orleans, Louisiana, USA, pp. 1246–1249.

[10] Plagwitz, H. et al. 2006, "A low-temperature passivation method for diffused phosphorus-as well as boron-emitters", *Proc. 21st EU PVSEC*, Dresden, Germany, pp. 688–691.

[11] Lauinger, T. et al. 1996, "Record low surface recombination velocities on 1 Ω cm *p*-silicon using remote plasma silicon nitride passivation", *Appl. Phys. Lett.*, Vol. 68, pp. 1232–1234.

[12] Schmidt, J. et al. 2004, "Recent progress in the surface passivation of silicon solar cells using silicon nitride", *Proc. 19th EU PVSEC*, Paris, France, pp. 391–396.

[13] Altermatt, P.P. et al. 2006, "The surface recombination velocity at boron-doped emitters: Comparison between various passivation techniques", *Proc. 21st EU PVSEC*, Dresden, Germany, pp. 647–650.

[14] Plagwitz, H. 2007, "Surface passivation of crystalline silicon solar cells by amorphous silicon films", Ph.D. thesis, Dept. Mathematics and Physics, Gottfried Wilhelm Leibniz Universität Hannover, Germany.

[15] Hofmann, M. et al. 2009, "Recent developments in rear-surface passivation at Fraunhofer ISE", *Solar Energy Mater. & Solar Cells*, Vol. 93, pp. 1074–1078.

[16] Ulyashin, A. et al. 2007, "Optical and passivation properties of double layer a-Si:H/SiN_x anti-reflective coatings for silicon solar cells", *Proc. 22nd EU PVSEC*, Milan, Italy, pp. 1690–1693.

[17] Gatz, S. et al. 2008, "Thermal stability of amorphous silicon/silicon nitride stacks for passivating crystalline silicon solar cells", *Appl. Phys. Lett.*, Vol. 93, p. 173502.

[18] Schmidt, J. et al. 2008, "Surface passivation of high efficiency silicon solar cells by atomic-layer-deposited Al_2O_3", *Prog. Photovolt: Res. Appl.*, Vol. 16, pp. 461–466.

[19] Schmidt, J., Veith, B. & Brendel, R. 2009, "Effective surface passivation of crystalline silicon using ultrathin Al_2O_3 films and Al_2O_3/SiN_x stacks", *physica status solidi* (RRL), Vol. 3, pp. 287–289.

[20] Veith, B. et al. 2011, "Comparison of the thermal stability of single Al_2O_3 layers and Al_2O_3/SiN_x stacks for the surface passivation of silicon", *Energy Procedia*, Vol. 8, pp. 397–312.

[21] Mäckel, H. & Lüdemann, R. 2002, "Detailed study of the composition of hydrogenated SiN_x layers for high-quality silicon surface passivation", *J. Appl. Phys.*, Vol. 92, pp. 2602–2609.

[22] Dauwe, S. 2004, "Low-temperature surface passivation of crystalline silicon and its application to the rear side of solar cells", Ph.D. thesis, Dept. Physics, Gottfried Wilhelm Leibniz Universität Hannover, Germany.

[23] Beyer, W. 2003, "Diffusion and evolution of hydrogen in hydrogenated amorphous and microcrystalline silicon", *Solar Energy Mater. & Solar Cells*, Vol. 78, pp. 235–267.

[24] Gatz, S. et al. 2012, "Firing stability of SiN_y/SiN_x stacks for the surface passivation of crystalline silicon solar

cells", *Solar Energy Mater. & Solar Cells*, Vol. 96, pp. 180–185.
[25] Seiffe, J. et al. 2011, "Surface passivation of crystalline silicon by plasma-enhanced chemical vapor deposition double layers of silicon-rich silicon oxynitride and silicon nitride", *J. Appl. Phys.*, Vol. 109, p. 034105.
[26] Sinton, R.A. & Cuevas, A. 1996, "Contactless determination of current–voltage characteristics and minority-carrier lifetimes in semiconductors from quasi-steady-state photoconductance data", *Appl. Phys. Lett.*, Vol. 69, pp. 2510–2512.
[27] Nagel, H., Berge, C. & Aberle, A.G. 1999, "Generalized analysis of quasi-steady-state and quasi-transient measurements of carrier lifetimes in semiconductors", *J. Appl. Phys.*, Vol. 86, pp. 6218–6221.
[28] Dullweber, T. et al. 2011, "Towards 20% efficient large-area screen-printed rear-passivated silicon solar cells", *Prog. Photovolt.*, DOI:10.1002/pip.1198.
[29] Herguth, A. et al. 2006, "Avoiding boron-oxygen related degradation in highly boron doped Cz silicon", *Proc. 21st EU PVSEC*, Dresden, Germany, pp. 530–537.
[30] Lim, B., Bothe, K. & Schmidt, J. 2008, "Deactivation of the boron–oxygen recombination center in silicon by illumination at elevated temperature", *physica status solidi* (RRL), Vol. 2, pp. 93–95.
[31] Gatz, S. et al. 2011, "19.4%-efficient large-area fully screen-printed silicon solar cells", *physica status solidi* (RRL), Vol. 5, No. 4, pp. 147–149.
[32] Gatz, S., Dullweber, T. & Brendel, R. 2011, "Evaluation of series resistance losses in screen-printed solar cells with local rear contacts", *IEEE J. Photovoltaics*, Vol. 1, pp. 37–42.
[33] Schmidt, J., Kerr, M. & Cuevas, A. 2001, "Surface passivation of silicon solar cells using plasma-enhanced chemical-vapour-deposited SiN films and thin thermal SiO2/plasma SiN stacks", *Semicond. Sci. Technol.*, Vol. 16 (2001), pp. 164–170.

About the Authors

Sebastian Gatz studied physics at universities in Regensburg and Dublin, and received his physics diploma from the Technical University of Munich in 2006. Since 2007 Sebastian has been a Ph.D. candidate at ISFH, where he is carrying out research on front- and rear-surface passivated screen-printed solar cells in the solar cell production processes group of Dr. Dullweber.

Jan Schmidt is head of the PV department at ISFH and professor of physics at LUH. He received his Ph.D. degree from LUH in 1998. Dr. Schmidt's current research interests include the analysis and manipulation of defects in silicon materials and the development of novel characterization techniques, as well as the development and evaluation of novel surface passivation methods for silicon solar cells.

Boris Veith studied physics at LUH and received his diploma degree in 2010. His thesis topic was a passivation method for silicon solar cells using aluminium oxide. Boris is currently employed as a scientist in the materials research group at ISFH, where he is involved with evaluating novel surface passivation methods for silicon solar cells.

Thorsten Dullweber leads the ISFH solar cell production processes research group, which focuses on process and efficiency improvements of industrial-type silicon solar cells. In particular, current research work includes the optimization of screen-printing processes, dielectric rear-surface passivation and high-rate aluminium evaporation.

Rolf Brendel is the scientific director of ISFH. He received his Ph.D. in materials science, specializing in infrared spectroscopy, from the University of Erlangen. Dr. Brendel's current research focuses on the physics and technology of crystalline silicon solar cells. Since 2004 he has been a full professor at the Institute of Solid-State Physics at LUH.

Enquiries

S. Gatz
Institute for Solar Energy Research Hamelin (ISFH)
Am Ohrberg 1
D–31860 Emmerthal
Germany

Tel: + 49 5151 999 314
Fax: + 49 5151 999 400
Email: s.gatz@isfh.de